

MODELING SiC/SiC COMPOSITES WITH OFF-AXIS FIBERS¹ – C. H. Henager, Jr. (Pacific Northwest National Laboratory², Richland, WA 99336, USA)

OBJECTIVE

This work updates modeling results for fiber composites having other orientations than 0/90. The work of Cox et al. has been used to derive a fiber bridging law for off-axis fibers that can be used to help model SiC/SiC composites fabricated into tubular geometries.

SUMMARY

A time-dependent fiber-bridging model that accounts for fiber orientation has been developed and its predictions are compared to strength and crack growth data for a braided weave composite. The level of agreement suggests that existing models of off-axis bridging fibers are not adequate for fusion reactor designs using SiC/SiC composites in off-axis orientations.

PROGRESS AND STATUS

Introduction

SiC is an excellent material for fusion reactor environments, including first wall plasma facing materials and breeder-blanket modules. In the form of woven or braided composites with high-strength SiC fibers it has the requisite mechanical, thermal, and electrical properties to be a useful and versatile material system for fusion applications [1-7]. The use of SiC-reinforced composites for fusion reactors or other nuclear applications will not be restricted to 0/90 aligned fiber architecture in all cases. It is important to understand the role of fiber orientation in the strength, toughness, and time-dependent properties for such materials. The use of high-strength ceramic fibers for composites is predicated on optimizing the strength, fracture resistance, and retained strength in aggressive environments, which argues for the best use of fiber strengths, namely on-axis loading for full load transfer to the high-strength fibers. Relatively few researchers have systematically studied the effects of fiber orientation on composite properties [8-10], and none have, to the best of our knowledge, performed any time-dependent testing of composites with off-axis or inclined fiber orientations.

Experimental Procedure

Materials tested

The SiC/SiC materials that were tested at PNNL are 1) a 5-harness satin weave, 8-ply, Hi-Nicalon Type-S fiber composite that was purchased in 2004 from GE Power Systems³ and 2) A Hypertherm⁴ composite purchased in 2006 that is $\pm 55^\circ$ braided weave, 10-ply plate, Hi-Nicalon Type-S fiber composite. The 5-harness satin weave 0/90 composite from GE Power Systems was manufactured for PNNL in 2002 with a bulk density of 2.69 g/cm³ and 40% nominal fiber volume fraction and was fabricated using isothermal chemical vapor infiltration (ICVI). A 150-nm thick pyrocarbon (PyC) interface was applied to the Type-S fibers prior to ICVI processing. The Hypertherm materials were also made with Type-S Hi-Nicalon fibers but coated with a 150 nm PyC, (100 nm CVI SiC, 20 nm PyC)₄ multi-layer interface applied prior to CVI matrix deposition. These materials had a nominal fiber volume fraction of 30%, a bulk density of 2.9 g/cm³, and a 380- μ m thick outer seal coat of SiC.

Mechanical property testing

¹ Poster presentation at ICFRM-13, Nice, FR, 2007.

² PNNL is operated for the U.S. Department of Energy by Battelle Memorial Institute under Contract DE-AC06-76RLO 1830.

³ <http://www.gepower.com>

⁴ Hypertherm HTC Inc. (Huntington Beach, Calif.)

The peak load fracture toughness, termed K_{Ic} , using single-edge notched beams (SENB) of each composite material was determined at ambient temperature and also at elevated temperature based on ASTM C-1421 (see Table 1).

Table 1: SENB Test Specifications

Composite Sample	Material-	Fixture ⁵		Sample		
		Support Span	Loading Span	Span (L)	Depth ⁶ (d)	Width (W)
0/90 5-harness satin weave – SENB ⁷		40	20	50	5	2.1
±55° braid – SENB ⁷		40	20	50	6.1	3.6

Model development

Analysis of bridging fibers aligned normal to the stress axes is well developed in the composite literature. We generally use shear-lag model with slip interface traction that results in a non-linear force displacement law. For non-aligned fibers we require a fundamentally different relation between force and displacement to account for fiber bending and so-called snubbing friction. Cox [8] has developed a force-displacement law that we will evaluate for off-axis ceramic fibers. Cox derived the following linear relation for fiber deflection due to bending and including snubbing friction effects:

$$W_{defl} = \frac{\mu_e \left[-\cos\phi + \cos(\theta_0 + \phi) + \frac{P \left(\frac{-P \cos\phi + e^{-\frac{\theta_0 \mu_e}{P}} (P \cos\phi - \mu_e \sin\phi)}{\mu_e} + \sin(\theta_0 + \phi) \right)}{\mu_e} \right]}{2r_f (P^2 + \mu_e^2) \tau_1} \quad (1)$$

where W is the fiber deflection, P is the force, ϕ is the fiber inclination angle, θ_0 is the bending angle, μ_e is the snubbing friction term, and τ_1 is the conventional sliding friction term. Plus, there is a term for elastic stretch of the fiber that is non-linear as before:

$$W_{el} = \frac{1 + e^{\frac{2\theta_0 \mu_e}{P}} (\mu_e - 1) \cos\phi}{8E_f r_f^2 \mu_e \tau_1} \quad (2)$$

Snubbing friction refers to the increase in friction as the inclined fiber is pulled and bends out of the ceramic matrix, much like the friction due to pulling a rope around a smooth edge. Such friction is highly localized but greatly modifies the fiber force-displacement law. The conventional force law is matched to the new force law when $\phi = 0$ as shown in Figure 1 and Figure 2 shows the new force law when ϕ is not equal to zero. In this case the bridging fiber becomes stiffer with increasing ϕ .

⁵ All dimensions are in mm in Table 1.

⁶ Sample surfaces in depth direction were left as received and were not polished.

⁷ a/W values were 0.16 for SENB samples.

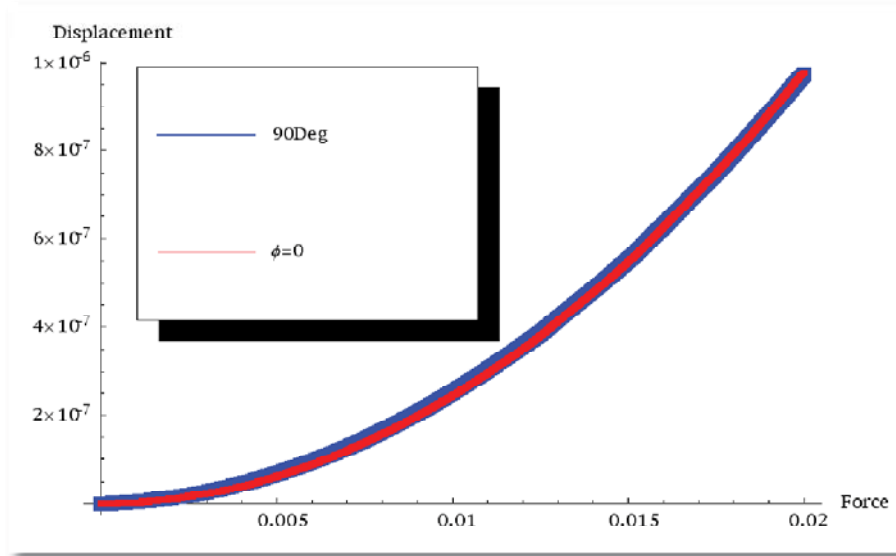


Figure 1. Force displacement law based on shear-lag model, denoted as 90 Deg curve, is matched to the new force law labeled $\phi = 0$ by adjusting μ_e and τ_1 in Eq. 2 since Eq. 1 is zero when $\phi = 0$.

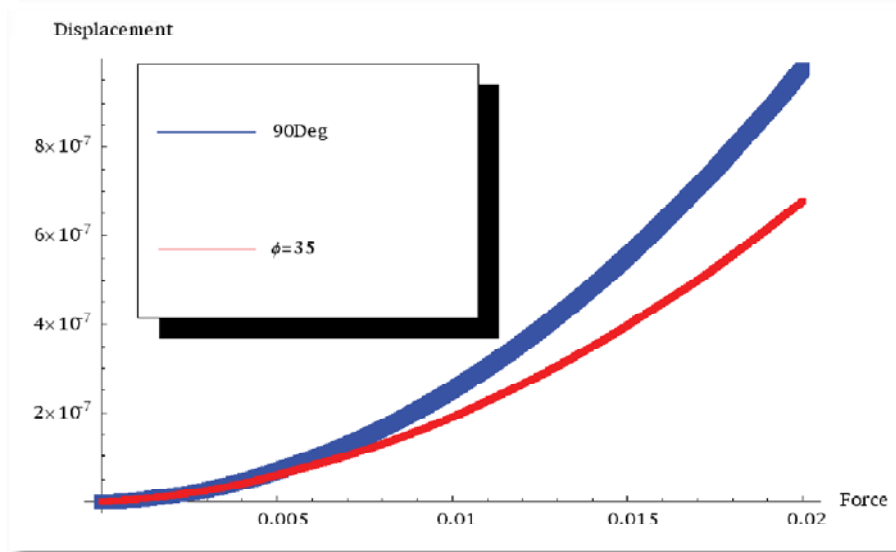


Figure 2. Force displacement laws are compared when ϕ is not equal to zero. With increasing ϕ the bridging force law decreases W_{el} and increases W_{defl} to give a “stiffer” bridge but now one that is part bending.

The bridging model requires a fiber stress function, which is constructed by partitioning the fiber force between tension and bending as:

$$\sigma_{br} = \frac{F_{br} \cos \phi}{2r_f} + \frac{3F_{br} \sin \phi M}{4r_f^2} \quad (3)$$

where the first term corresponds to our previous tensile orientation stress when $\phi = 0$ and the second term is the bending term accounting for the moment of inertia for a 2D bridge in our model [11]. We can

put a lower bound on M using the COD but M may be larger than that due to interactions with the SiC matrix that act to increase the moment arm. In the new model, F_{br} is calculated using Eqs. 1 and 2 based on the fiber deflection required to remain a bridging fiber in the dynamic crack bridging model [11]. We then make use of Eq. 3 to compute the stress on the bridging fiber to track fiber failure as a function of fiber displacement, which now includes bending due to fiber inclination angle.

Results

Figure 3 shows the results of the SENB toughness measurements, reported as K_{Ic} , for each material. The braided weave material has a fracture toughness of approximately one-third of that of the 0/90 composite. Can we rationalize this data with the Cox bridging model that we have constructed? Our tensile bridging model predicts fracture toughness quite accurately using typical composite data and average fiber strength of 2.5 GPa. If we use those parameters and vary the fiber inclination angle according to our implementation of the Cox equations, then we predict the following, where $\phi = 35^\circ$ as defined by Cox. In Figure 4 we show the results of these calculations for inclined fiber composites based on our implementation of the Cox model. Three cases are shown in Figure 4, including no snubbing friction, a snubbing friction ratio of 200:1 relative to the interfacial shear friction term, and snubbing, plus a doubling of the fiber bending moment due to matrix spallation during fiber deformation and bending.

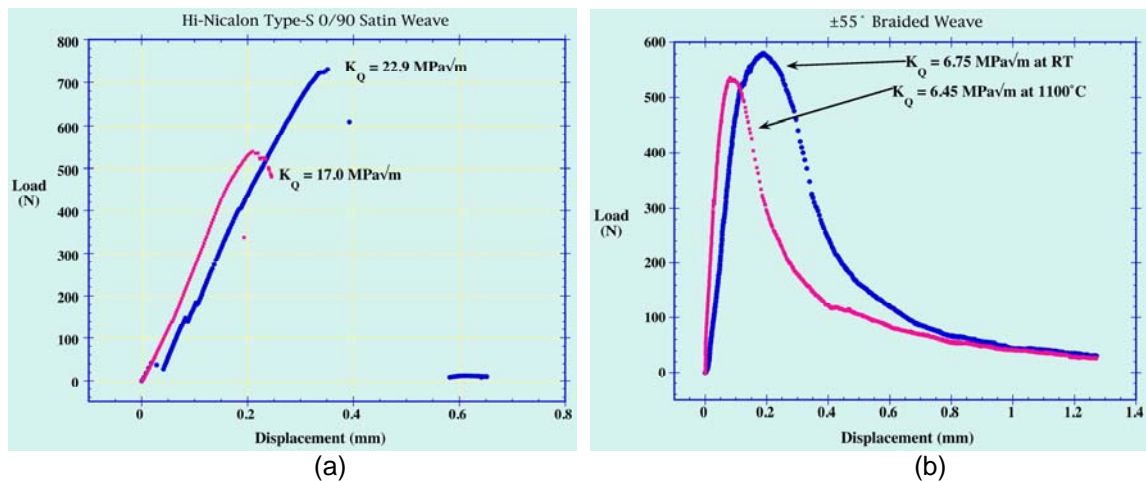


Figure 3. SiC-composite fracture toughness, K_{Ic} , for (a) 0/90 satin-weave material and (b) ±55 braided weave material showing the large difference in measured toughness at ambient and at 1373K.

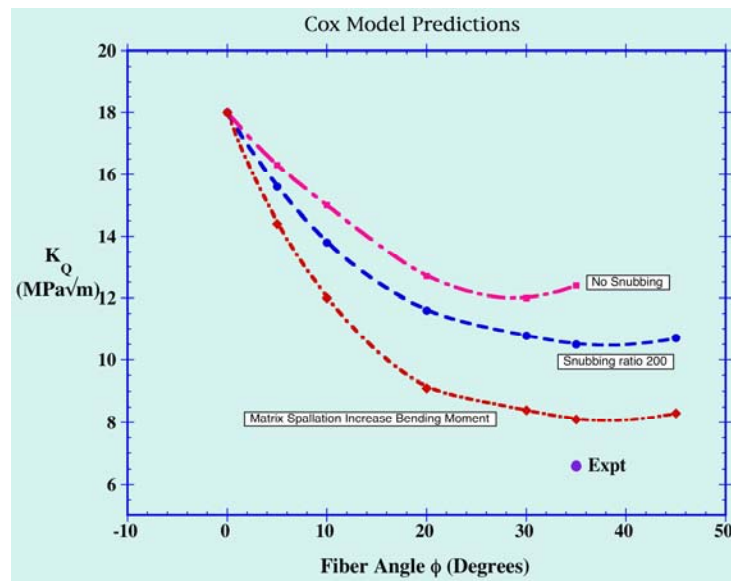


Figure 4. Predicted fracture toughness as a function of fiber inclination angle using a fiber strength of 2.5 GPa, which is the same strength used in our model for 0/90 oriented composites. The experimental data point lies below all three curves.

In general, the model cannot account for the observed decrease in toughness due to fiber inclination. This suggests either a refinement to the model is required or that more data should be obtained on composites with similar fiber volume fractions and processing conditions. However, microstructural observations help support some of the model assumptions. Matrix spallation is observed which complicates the determination of the bending moment that a fiber experiences. Figure 5 shows SEM images of fiber fractures from the braided weave composite material illustrates matrix spallation as evidenced by the exposed fiber channels and apparent shear failure of the fracture fibers as evidenced by the fracture inclination angle.

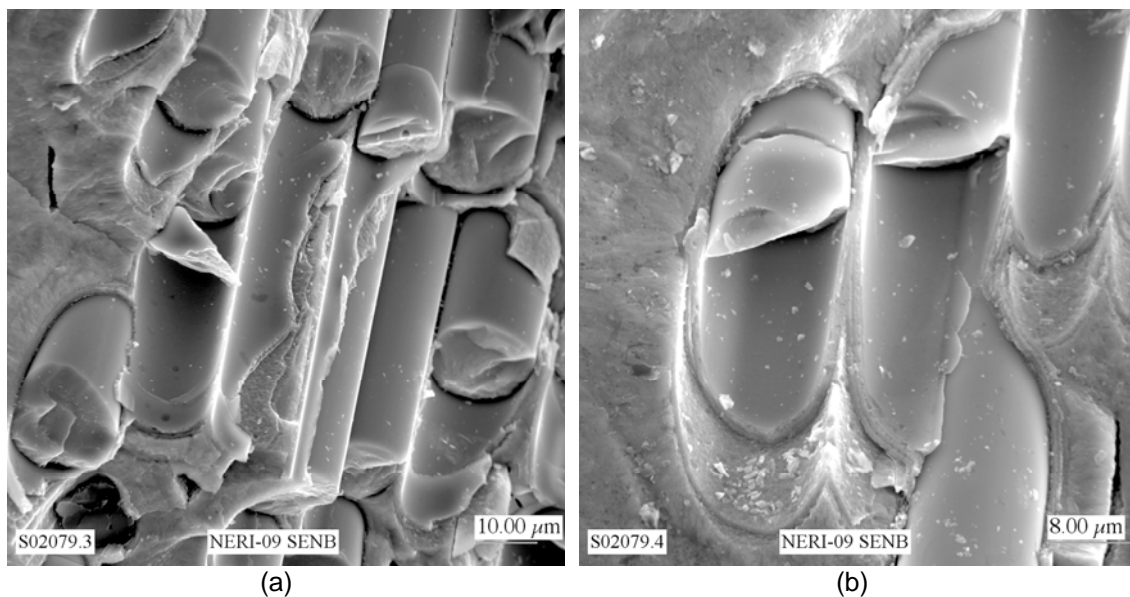


Figure 5. SEM micrographs of ± 55 braided weave fracture surfaces showing matrix spallation and fiber shear fracture features. In (a) and (b) we observe fiber channels exposed due to spallation. In (b) we observe fiber shear fracture features.

Conclusions

A new force displacement law for inclined bridging fibers in SiC/SiC composites has been developed based on a model by Cox for the force required to pull out an inclined fiber from an elastic matrix. The modified fiber-bridging model is not able to fully account for observed fracture toughness data for a braided fiber composite. Additional data is required to further test the model. Several critical model assumptions, however, were verified by fractography.

References

- [1] Y. Katoh, L.L. Snead, C.H. Henager Jr, A. Hasegawa, A. Kohyama, B. Riccardi and H. Hegeman, J. Nucl. Mater. 367-370 A 659 (2007).
- [2] C.H. Henager, Jr., Y. Shin, Y. Blum, L.A. Giannuzzi, B.W. Kempshall and S.M. Schwarz, J. Nucl. Mater. 367-370 1139 (2007).
- [3] S.J. Zinkle, Fusion Engineering and Design 74 31 (2005).
- [4] J.B.J. Hegeman, J.G. Van Der Laan, M. Van Kranenburg, M. Jong, D. D'Hulst and P. Ten Pierick, Fusion Engineering and Design 75-79 789 (2005).
- [5] Y. Katoh, A. Kohyama, T. Hinoki and L.L. Snead, Fusion Science and Technology 44 155 (2003).
- [6] R.H. Jones, L. Giancarli, A. Hasegawa, Y. Katoh, A. Kohyama, B. Riccardi, L.L. Snead and W.J. Weber, J. Nucl. Mater. 307-311 1057 (2002).
- [7] Y. Katoh, T. Nozawa, L.L. Snead, T. Hinoki and A. Kohyama, Fusion Engineering and Design 81 937 (2006).
- [8] B.N. Cox, Mechanics of Advanced Materials and Structures 12 85 (2005).
- [9] D.D.R. Cartie, B.N. Cox and N.A. Fleck, Composites Part A: Applied Science and Manufacturing 35 1325 (2004).
- [10] B.N. Cox and N. Sridhar, Mechanics of Advanced Materials and Structures 9 299 (2002).
- [11] Henager C.H, Jr. and R.G. Hoagland, Acta Mater. 49 3739 (2001).